

Divergent Clinical Equivalence Findings from DVH and NTCP Metrics for Alternative OAR Delineations with Increasing Setup Variability in Head-and-Neck Radiotherapy

M.N.H. Rashad,^{1,*} Abishek Karki,¹ Jason Czak,¹ Victor Gabriel Alves,¹ Hamidreza Nourzadeh,² Wookjin Choi,² and Jeffrey V Siebers¹

¹*University of Virginia, Charlottesville, VA, 22903*

²*Thomas Jefferson University, Philadelphia, PA, 19107*

(Dated: August 14, 2024)

Purpose: This study quantifies the variation in dose-volume histogram (DVH) and normal tissue complication probability (NTCP) metrics for head-and-neck (HN) cancer patients when alternative organ-at-risk (OAR) delineations are used for treatment planning and for treatment plan evaluation. We particularly focus on the effects of daily patient positioning/setup variations (SV) in relation to treatment technique and delineation variability.

Materials and Methods: We generated two-arc VMAT, 5-beam IMRT, and 9-beam IMRT treatment plans for a cohort of 209 HN patients. These plans incorporated five different OAR delineation sets, including manual and four automated algorithms. Each treatment plan was assessed under various simulated per-fraction patient setup uncertainties, evaluating the potential clinical impacts through DVH and NTCP metrics.

Results: The study demonstrates that increasing setup variability generally reduces differences in DVH metrics between alternative delineations. However, in contrast, differences in NTCP metrics tend to increase with higher setup variability. This pattern is observed consistently across different treatment plans and delineator combinations, illustrating the intricate relationship between SV and delineation accuracy. Additionally, the need for delineation accuracy in treatment planning is shown to be case-specific and dependent on factors beyond geometric variations.

Conclusions: The findings highlight the necessity for comprehensive quality assurance programs in radiotherapy, incorporating both dosimetric impact analysis and geometric variation assessment to ensure optimal delineation quality. The study emphasizes the complex dynamics of treatment planning in radiotherapy, advocating for personalized, case-specific strategies in clinical practice to enhance patient care quality and efficacy in the face of varying SV and delineation accuracies.

I. INTRODUCTION

Organ-at-risk (OAR) delineations used for radiotherapy treatment planning are assumed to represent the true underlying structure. However, inter-observer, intra-observer, and inter-algorithm OAR delineation variations [1–5] indicate that clinical delineations are not absolutely accurate. Nonetheless, decades of successful radiotherapy have shown that absolute accuracy is not required.

OAR delineation accuracy requirements depend on factors such as proximity to the target, treatment technique, and the OAR dose-response characteristics. Additionally, inter-treatment patient setup variability and organ motion/deformation affect the OAR dose, hence influencing the required delineation fidelity.

Comparisons of alternative manual delineations (MDs) in standardization studies [6] and between MDs and auto-delineations (ADs) based on geometric indices [7–9] do not assess their adequacy for treatment planning. Some studies quantify the dosimetric effect of alternative delineations post-planning [10, 11], but post-planning evaluation does not evaluate their suitability for treatment planning. Delineation variations can significantly impact patient treatment [12].

Recent investigations recognize the need to utilize alternative test delineations in the treatment planning process, and explore correlations between geometric indices and dosimetric variations, revealing complex and case-specific relationships. [13–15] Some studies [16, 17] demonstrate adequacy of ADs for treatment planning; others [18, 19] find substantial dose differences despite minor geometric variations. These studies generally utilized few (10-20) patients, a single treatment planning technique, and/or few (e.g. 2) alternative delineation sets.

This study examines if/how daily patient setup variations affect the clinical impact of alternative delineations in radiation therapy planning. Our work builds on previous approaches by using a large (209) patient cohort, five alternative delineations, three treatment planning techniques. We examine the interplay between delineation variability and daily patient setup variations, evaluating potential clinical effects using D_{\max} , D_{mean} , and normal tissue complication probability (NTCP). This comprehensive approach aims to understand how these factors collectively influence the clinical impact of alternative delineations in radiation therapy planning.

* Email: hashir@virginia.edu

II. MATERIALS AND METHOD

For each patient in a 209 head and neck (HN) patient dataset, 2-arc VMAT, 5-beam and 9-beam IMRT treatment plans were created using five alternative OAR sets (one MD, four AD) using an unsupervised auto-planning algorithm. The same MD targets were used for all treatment plan optimizations. Each treatment plan was evaluated with each alternative OAR set under six different patient setup uncertainty scenarios. The potential clinical impact of using alternative structure sets was assessed using DVH and NTCP plan quality indices (PQI). The ΔPQI between planning and alternative OAR set evaluations were compared to clinical tolerances, below which the delineations are considered equivalent. Differences and similarities in the effects of increasing setup variation on equivalence for D_{mean} , D_{max} , and NTCP PQI s for the different OARs and beam arrangements were evaluated.

A. Data curation

Two-hundred nine HN datasets from two The Cancer Image Archive (TCIA) collections were used in this study. Seventy three were from Head-Neck Cetuximab collection [20, 21], and 136 were from Head-Neck-PET-CT [22, 23] collection.

Most CT images and manual OAR delineations (187) were sourced from the UaNet Github repository [24], which curated the delineations [25]. UaNet Dataset 2 includes 140 CT scans from the TCIA Head-Neck Cetuximab [20] and Head-Neck-PET-CT [22] collections, with up to 28 OARs per patient re-delineated by a single experienced radiation oncologist and reviewed by a second expert [25, 26]. One dataset 2 patient was excluded due to miss-alignment of the PTVs with the CT image set. UaNet Dataset 3 from the Public Domain Database for Computational Anatomy (PDDCA - Version 1.4.1), includes 48 CTs with up-to 9 manually delineated OARs from the Head-Neck Cetuximab collection [20] which were re-segmented for use in the 2015 Head and Neck Auto Segmentation MICCAI Challenge [8]. The remaining 22 patients were processed in-house from the Head-Neck-PET-CT [22] collection. For all patients, PTVs were selected from the TCIA collections. Patients in the dataset were limited to those from which we could discern an unambiguous association between the CTs and the corresponding aligned contour sets.

Auto-delineations for each CT image set were created using AutoContour (Radformation Inc [27]), INTContour (Carina Inc [28]), Syngo.via (Siemens Healthineers) and SPICE (Pinnacle, Philips Professional Healthcare), referred to as AD1, AD2, AD3, and AD4. All auto-delineations were used without modification to ensure delineation variability, with grossly erroneous delineations eliminated through geometric comparisons.

Figure 1 compares the alternative delineations of four

OARs for four patients illustrating variations in the alternative delineations.

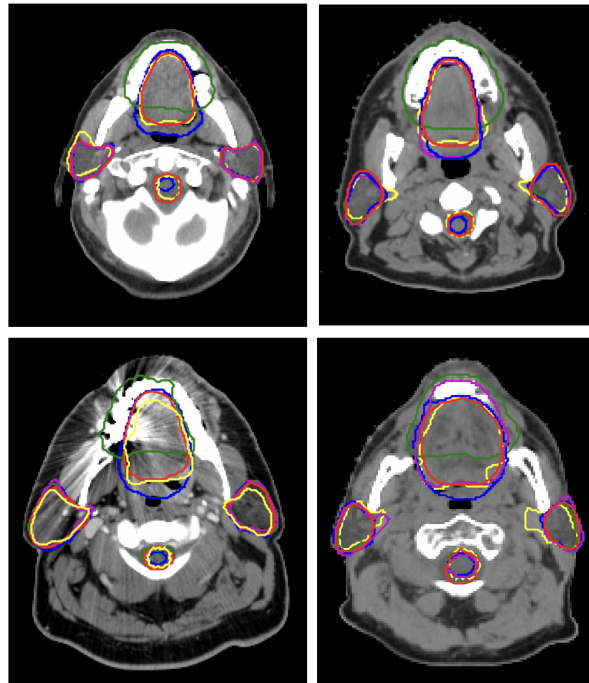


FIG. 1. Examples of the variability observed between the alternative delineations (manual and auto) for four different patients. Only SpinalCord, Parotid_L, Parotid_R and Cavity_Oral are shown for clarity. The contours colors are, MD=Manual: Magenta, AD1=Radformation: Red, AD2=Carina: Green, AD3=Siemens: Blue and AD4=SPICE: Yellow. The observed DV is patient and OAR specific.

B. Geometric comparisons

Volumetric Dice Similarity Coefficient (vDSC) and robust Hausdorff Distance (HD95) geometric indices (GIs) were computed for all OAR and delineator combinations using methods from Alphabet Inc. Google DeepMind [29]. GIs were used for first-order delineation quality assurance and to evaluate correlations between geometric and dosimetric differences. For dosimetric and NTCP analysis, delineation pairs with $vDSC < 0.5$ were excluded. For the SpinalCord, geometric comparisons were limited to CT slices common between both delineators, which we define as "common-slice-Dice".

C. Treatment plan creation

Two-arc VMAT, 5-beam IMRT and 9-beam IMRT plans were created for each patient using the MD targets and each alternative structure set, totaling 15 plans

per patient (3135 plans in total) with the auto-planning algorithm in Pinnacle 16.2. All patients used the same base PTV prescription dose-levels, 70, 63 and 56 Gy in 35 fractions, regardless of the clinical plan dose level. For Patients with <3 PTVs, the prescription limited to the highest dose level PTVs. Using higher-than-clinical dose levels was a conservative approach as it results in higher OAR doses and higher sensitivity to delineation variations. Each plan was optimized for the same base objectives (Table I). OARs not present in a delineation set were excluded from that optimization. Differences in optimization OAR set minimally affected the validity delineation equivalence assessments (section II F), as the missing OAR was then excluded from the pair-wise analysis.

OAR Name	Optimization Objectives					NTCP Parameters			
	Dmax (Gy)	Dmean (Gy)	DVH_V (Max %)	DVH_D (Max Gy)	Priority	n	m	TD_{50}	End Point
BrachialPlexus (L&R)	66	-	3	62	Low	-	-	-	-
Brainstem	54	-	5	52	High	0.16	0.14	65	Necrosis/infraction
GlnD_Submands (L&R)	-	35	-	-	High	0.70	0.18	46, 56	Xerostomia
Larynx	63	-	3	39	High	-	-	-	-
Bone_Mandible	75	-	-	-	High	0.07	0.10	72	Marked limitation of joint function
OpticChiasm	44	-	-	-	High	-	-	-	-
OpticNrv (L&R)	55	-	-	-	High	-	-	-	-
Parotid (L&R)	-	26	7	20	High	0.70	0.18	46	Xerostomia
SpinalCord	45	-	-	-	High	0.05	0.175	66.5	Myelitis/necrosis
Trachea	69	-	5	60	High	-	-	-	-

TABLE I. Describes the optimization objectives used in the study by the auto-planning algorithm and NTCP parameters, n , m and TD_{50} used in the study. These parameters (except for GlnD_Submands) are obtained from [30]. For GlnD_Submands, we used the same parameters as the Parotid as well as a slightly elevated TD_{50} .

D. Setup variability (SV) simulation - RTRA

To understand the effects of alternative delineations amidst inherent treatment uncertainties, including patient setup uncertainties, we used the Radiation Treatment Robustness Analyzer (RTRA) [5] to simulate the impact of setup uncertainties on the planned dose distribution, dose-metrics, and normal tissue complication probability (NTCP).

RTRA simulates OAR setup uncertainties using rigid body translations in the left-right, anterior-posterior, and superior-inferior directions. These translations are sampled from zero-centered normal distributions with user-set standard deviations for random (per fraction) (σ) and systematic (per treatment course) (Σ) uncertainties. The translated OARs are combined with the planned dose to evaluate dose volume histograms (DVH) and dose volume coverage map (DVCM) [31] for 1000 treatment course simulations. The DVHs and DVCMs are then used to compute probabilistic $PQIs$, assessing the probability of achieving a given PQI , with evaluations at the 95% confidence level.

To assess the effect of setup uncertainty on the $PQIs$, we simulated setup uncertainties with $\sigma = \Sigma \in [0, 2, 4, 6, 8, 10]$ mm. These values range from the static plan (0 mm) to various clinical setup uncertainties, in-

cluding IGRT-based setups, laser-based setups, and extending to clinically unrealistic large uncertainties.

The largest simulated uncertainty, while extending beyond typical clinical scenarios, enabled us to quantify trends in the PQI assessments. This comprehensive analysis helped determine if and when setup variability outweighs delineation uncertainty, providing an understanding of whether permissible delineation variability depends on the setup uncertainty.

E. Normal tissue complication probability (NTCP)

For a given OAR, delineator, and simulated setup uncertainty, NTCPs were computed using the Lyman-Kutcher-Burman (LKB) model [30] for each of the 1000 treatment course simulations per SV level. Table I lists the n (volume-effect parameter), m (dose-response slope) and TD_{50} (uniform irradiation dose resulting in 50% complication) used from [30].

$$NTCP = \frac{1}{\sqrt{2\pi}} \int_{-\infty}^t e^{-\frac{x^2}{2}} dx \quad (1)$$

$$t = \frac{EUD - TD_{50}}{mTD_{50}}, \quad (2)$$

with, equivalent uniform dose EUD equal to the generalized mean dose gMD [32] computed from RTRA computed differential DVHs dose-volume pairs $\{D_i, v_i\}$ for each treatment course Niemerko's DVH reduction scheme [32].

$$EUD = gMD = \left(\sum_i v_i D_i^{1/n} \right)^n \quad (3)$$

Although the analysis was performed for all organs listed in Table I, results are presented only for the Spinal-Cord, (a serial organ whose response is proportional to the maximum dose), and the Parotids, (a parallel organ whose response is proportional to the mean dose). Parotid glands were separated into those intersecting a PTV and those that do not.

F. Delineation equivalence assessment

For brevity, we define the planning delineation (PD) as the delineation set used for the treatment plan creation, and test delineation (TD) as the delineation set used for plan evaluation. When the TD-based evaluation meets the plan objectives, the PD OARs were adequate for the task of plan creation when TD represents the true underlying organ.

We quantify delineation equivalence by the difference in the PDI between the plan evaluated with the same structure set ($PD(A)$) used for plan creation (PQI_{AA}) ($PD=TD$) and the plan evaluated with an alternate structure set B (PQI_{AB}) ($PD\neq TD$).

$TD(B)$ is clinically equivalent to $PD(A)$ if

$$\Delta PQI_{AB} = |PQI_{AA} - PQI_{AB}| < C_{Tol} \quad (4)$$

where C_{Tol} is the clinical tolerance.

Reversing the roles of PD and TD structure sets (structure set B used for plan creation and structure set A for plan evaluation) evaluates ΔPQI_{BA} , the clinical equivalence of $TD(A)$ with $PD(B)$.

Since reversing these roles results in a different optimized dose distribution, generally, $PQI_{AA} \neq PQI_{BB}$, $PQI_{AB} \neq PQI_{BA}$, and $\Delta PQI_{AB} \neq \Delta PQI_{BA}$. Hence, joint equivalence of A and B requires,

$$\text{Max}(\Delta PQI_{AB}, \Delta PQI_{BA}) < C_{Tol} \quad (5)$$

While a two-way assessment is necessary to establish full delineation equivalency, a one-way assessment is sufficient to demonstrate that plans created with PD are adequate when TD represents the underlying organ, even though the reversal of the PD and TD may result in clinical non equivalency.

Delineation equivalence assessments were computed for each (TD, PD) pair for each treatment plan. With 5 delineators, we performed 4 assessments per PD and 20 one-way assessments in total per plan. Considering 3 treatment planning techniques, we have 60 total one-way assessments per patient for each level of setup uncertainty. Assessments without considering the effects of setup variability (equivalent to $\sigma = \Sigma = 0$) and those including setup variability were computed.

III. RESULTS

A. Relationship between geometric and dosimetric variations

Figure 2 shows the vDSC HD95 values for the combined Parotids (Parotid_L + Parotid_R) for each PD-TD pair. All structures and delineator pairs had a median $HD95 \leq 0.8$ mm and median $vDSC \geq 0.8$. With the exception of the AD4 contours, few delineations had $vDSC \leq 0.5$ or $HD95 \geq 15$ mm. For delineations with $vDSC \leq 0.5$, one delineation in the comparison pair is labeled erroneous.

The correlation of geometric indices (GI) with ΔPQI_{AB} , excluding the effect of SV (for $\Sigma = \sigma = 0$ mm), is shown in Figure 3 for Parotids' $\Delta D_{\text{mean}, AB}$ (Gy) and $\Delta NTCP_{AB}$ (%) for the combination of AD1 and AD2 delineations with the 2arc VMAT plans. While weak correlation are discernible, large vari-

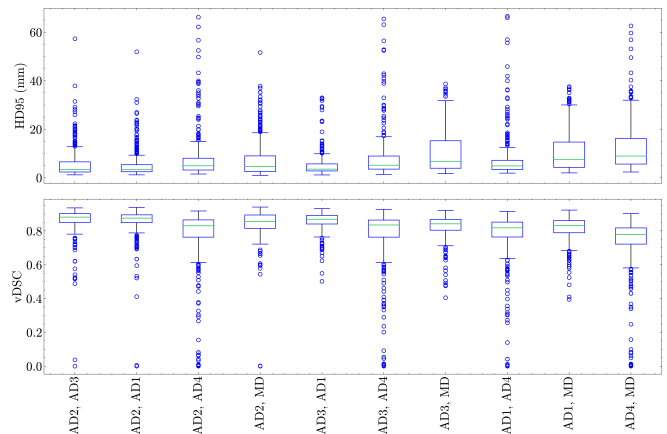


FIG. 2. Distribution of HD95 in mm (top) and vDSC (bottom) for Parotids (Left + Right) for all of the delineator combinations. The vast majority of delineations had vDSC greater than 0.8. Note, cases with $vDSC < 0.5$ were excluded from the dosimetric analysis. Geometric differences were greatest for comparisons involving delineator AD4, a model-based auto-delineation method.

ations in ΔD_{mean} (Gy) and $\Delta NTCP$ (%) for the same GI, along with the existence of small dose and $NTCP$ deviations despite large geometrical differences suggests that the delineation accuracy required for treatment planning is case-specific and depends on factors beyond simple geometrical variations. Similar weak correlations (not shown) are observed for other OARs and for the 5- and 9-beam plans. This indicates that a comprehensive delineation QA program should consider dosimetric impact analysis in addition to geometrical variation analysis.

B. Effect of setup variability on clinical impact of DV

To assess the effect of setup variability on delineation variability, we present the results of the union of one-way assessments between PD, TD pairs ($\Delta PQI = \Delta PQI_{AB} \cup \Delta PQI_{BA}$). Our overall remain consistent whether we consider one-way assessments, the union of one-way assessments, or two-way assessments. While we restricted our presented results to PD-TD pairs which have $vDSC \geq 0.5$, including $vDSC < 0.5$ yields similar observations as discussed below.

1. Qualitative assessment

Equation 5 outlines the criterion used to evaluate the clinical equivalency of alternate delineations. Instead of using a fixed C_{Tol} value, we analyse the cumulative distribution function (CDF) of ΔPQI to assess equivalency as a function of C_{Tol} , demonstrating the robustness of our findings to C_{tol} .

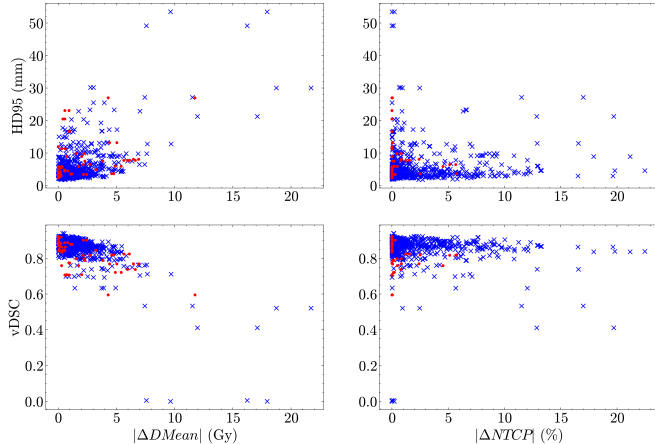
HD95, vDSC vs $|\Delta D_{Mean}|$ and $|\Delta NTCP|$ 

FIG. 3. Relationship between the geometric indices for alternative Parotid (L+R) delineations and the ΔD_{mean} (Gy) (left column) and $\Delta NTCP$ (%) (right column) for AD1 and AD2 combinations for all patients for the 2arc VMAT plans. Top row: HD95, bottom row: volumetric DSC. The Δ 's were evaluated for the static plans (no SV simulated). Parotids which overlap with a target volume are shown in blue. Those with overlap, are in red.

Figure 4 compares the alternative delineations, including the effect of varying amounts of SV for SpinalCord (Serial - MaxDose organ) and Parotids (Parallel - MeanDose organ) as evaluated by ΔDVH_{95} and $\Delta NTCP_{95}$ metrics. Each series shows the behavior of ΔPQI as a function of the simulated SV. On the CDFs, the Y value at a given $\Delta PQI = C_{tol}$ on the X axis indicates the number of in-tolerance (equivalent) delineations. Conversely, for a given nROI on the Y, the X value gives the associated C_{tol} . This enables us to infer the behavior of equivalency at a series of tolerance values.

The observations can be summarized as follows,

- Increasing SV generally increases the number of equivalent OARs for all DVH Metric evaluations, indicating a washout effect, except for non-overlapping parotids, where increasing SV decreased the number of equivalent OARs.
- Increasing SV decreases the number of equivalent alternative OARs decreases when evaluated using NTCP for all OARs except for GlnD_Submands, which washout effects for both DVH and NTCP.
- These trends were consistent across all planning techniques and delineator combinations studied.

These differences in the effect of SV on the impact of DV, as measured by DVH Metric vs NTCP, suggests that DVH Metrics may be poor proxies for clinical effect, similar to the findings of [35]. This supports the TG 166 recommendation to use biologically related models for

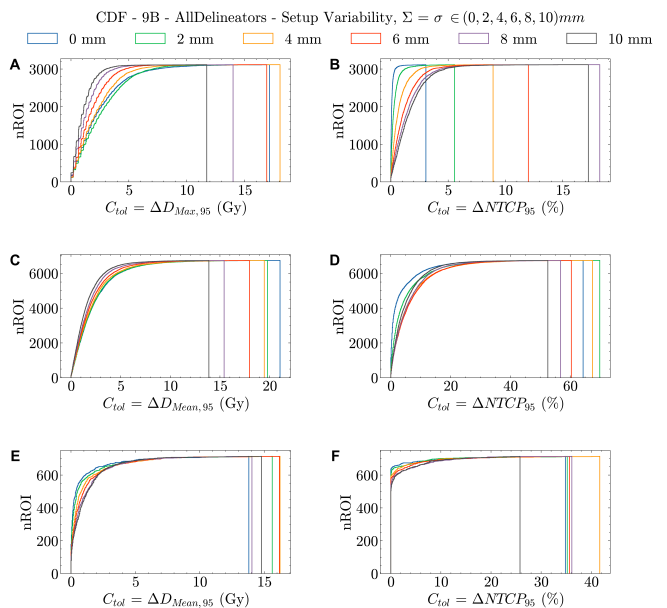


FIG. 4. Cumulative histograms of the union of ΔPQI_{AB} for $A, B \in MD, AD1, AD2, AD3, AD4$ with $A \neq B$, showing the number of delineations with $\Delta PQI < C_{tol}$ for different simulated setup variabilities (SV). ΔPQI s are evaluated at the 95% confidence level. Each data series shows the number of equivalent delineations (A) CDF of SpinalCord $\Delta D_{Max,95}$, indicating an increase in equivalent delineations with increasing SV. (B) CDF of SpinalCord $\Delta NTCP_{95}$, showing an increase in $\Delta NTCP_{95}$ with increasing SV. (C) and (D) show similar trends for Parotid Glands overlapping with the target (E) and (F), however, show a decrease in equivalent delineations with increasing for non-overlapping Parotids. The plot is for 9-beam IMRT plans, consistent with 5-beam and 2-arc plans.

treatment planning [36, 37] and highlights the need to consider an endpoint metric such as NTCP in any dosimetric impact analysis to determine required delineation quality.

2. Quantitative assessment

The CDFs in Figure 4 are from ΔPQI_i evaluations for each $i \in 2 \times n_{ROIs}$ from the $A = MD, B = AD1$ evaluations.

Defining the equivalency fraction as

$$F_{eq} = \frac{nROI(\Delta PQI \leq C_{tol})}{nROI_{total}} \quad (6)$$

allows evaluation of the C_{tol} to achieve a given fixed F_{eq} as a function of SV as CDFs. Uncertainties in the CDFs were obtained using bootstrap sampling [38, 39] with replacement using the 209-patient sample. The median C_{tol} for each $F_{eq} \in (0.5, 0.8, 0.9)$ and its 68% confidence range were computed. Decreasing C_{tol} with increasing SV indicates a decreased clinical effect, while increasing

C_{tol} suggests an enhanced clinical effect with alternative delineations.

Figure 5 shows results for $F_{eq} = 0.9$ for the 2-arc plans and SpinalCord ($PQI \in (D_{max}, NTCP)$). The negative slope in SV vs. C_{tol} for D_{max} evaluations indicates a washout effect, consistent with Aliotta et al. [40]. Conversely, the positive slope in the NTCP evaluations indicates increased clinical effect of DV with SV.

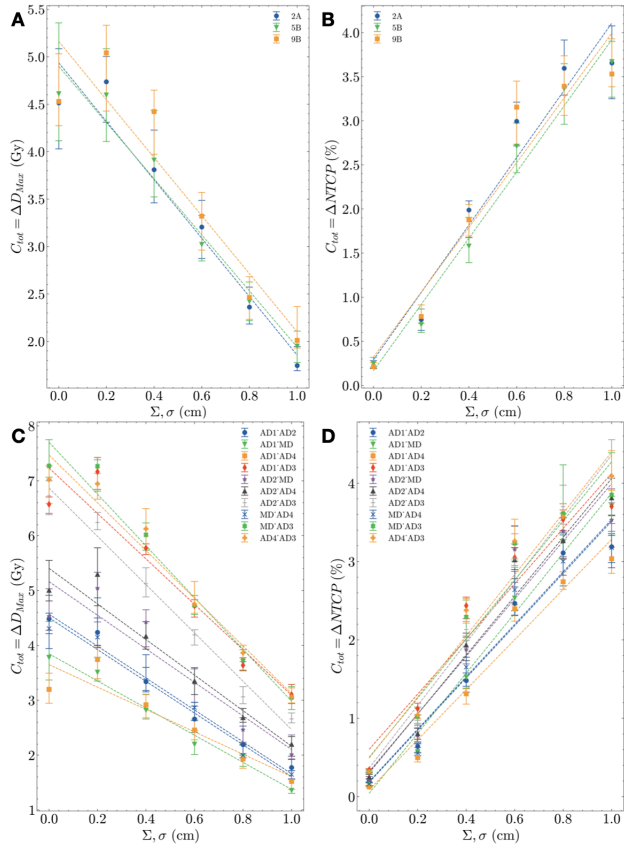


FIG. 5. C_{tol} for $F_{eq} = 0.9$ for SpinalCord delineations with each simulated setup uncertainty level. Bootstrap sampling with 10000 iterations was used to account for the sampling uncertainty. The median ΔPQI , and the 68% confidence level are reported. Dotted lines represent the weighted linear fit. (A) and (B) compare different planning techniques with a fixed PD-TD combination (MD & AD2) for ΔD_{max} and $\Delta NTCP$ respectively. Different PD-TD combinations for a fixed planning technique (9B) are compared in (C) and (D).

Figure 5(A) and (B) compare the 3 treatment planning beam arrangements for $F_{eq} = 0.9$ and SpinalCord. Increasing SV reduces the impact of DV for the DVH metric but it increases it for NTCP across all planning techniques. Panels (C) and (D) compare of the effect of SV for different PD-TD combinations for SpinalCord, showing similar trends. Differences measured using dose-based PQIs between PD-TD combinations are larger than those observed from NTCP for clinically rel-

evant setup variabilities (0mm-4mm).

IV. DISCUSSION

While some previous studies found significant differences in dose-based PQI s evaluated on alternative delineations when evaluated on the static treatment plan [18, 19], when inherent SV is considered, Aliotta et al. [40] found that dose-based PQI differences decreased as simulated SV increased. Our results align with these findings (except for non-target-overlapping parotids); ΔD_{mean} and ΔD_{max} values from alternative delineations decreased with increasing simulated SV. However, NTCP differences increases with SV (except for the GlnD_Submands).

Previous studies reported weak correlation between GIs and dosimetric changes for alternative delineations [15, 18, 19], indicating that GIs are inadequate for determining the clinical adequacy of delineations [41]. Our findings support those conclusions. However, these conclusions are from prioritizing PTV coverage over OAR sparing. If OAR sparing was prioritized over PTV coverage (as in lung trials), then the sensitivity to geometric changes could be higher.[42].

In preliminary testing, the auto-planning algorithm terminated with high (>55 Gy) SpinalCord D_{max} for some patients. These plans, which would never be used clinically, had particularly high sensitivity of $\Delta NTCP$ to increasing SV even though ΔD_{max} reduced with increasing SV. This is due to the large slope of the sigmoidal NTCP curve at large D_{max} values. Final auto-plans reduced the SpinalCord D_{max} (to <55 Gy), and reduced, but did not eliminate this effect.

To ensure the delineations used differed, extensive delineation review and adjustment by medical experts was not performed in this study, even though adjustment of AI contours improves their geometric conformance to manual delineations [9], the reported improvements are small (average vDSC improvement 0.02 ± 0.02). Thus, our delineation variations may be greater than clinical practice, but this is unlikely to affect our conclusions.

Delineations excluded for $vDSC < 0.5$ had outlier ΔPQI s values and were often clearly erroneous (e.g. an AI SpinalCord miss-placed to the posterior skull). Additionally, a few (MD SpinalCord) delineations were missing slices, which was corrected for by interpolation prior to planning.

Visual inspection revealed systematic differences between some delineation sets. For instance, one AD set SpinalCord encompassed the entire spinal canal, while other conformed to the SpinalCord. Despite this, equivalence evaluations followed the same trends for this set.

Using common dose levels and auto-planning techniques may have added clinically conservative aspects to our study. While clinically, different dose levels are used based on the primary disease and nodal involvement, we consistently used 70 Gy, yield higher doses to

OARs. Similarly, our lack of beam or collimator angle optimization for our 5-beam, 9-beam, and 2-arc VMAT plans also contributed to conservatively high OAR doses, as did the lack of post-auto-planning dosimetrist tuning to provide additional OAR protection.

Our dataset had a low fraction (8%) of parotids not overlapping with target volumes. For these parotids, the $\Delta D_{\text{mean},95}$ increased as the simulated SV increased with SV, unlike overlapping parotids and other OARs. The non-overlap parotids SV dependence is due to the dose blurring-effect of random SV moving dose from the adjacent high-dose regions into the parotid.

Differences in SV effects between (ΔD_{max} , ΔD_{mean}) and $\Delta NTCP$ stresses the need to focus on clinical effects, rather than just dose-metrics. Large dose-metric changes can be clinically inconsequential for NTCP, while small changes near dose-metric tolerance can significantly change NTCP. Cases where DV alone caused a dose metric violation occurred in less than 1% of the cases studied.

V. CONCLUSION

Our study highlights the complex interplay between SV and DV in radiotherapy planning. We found that increasing SV generally reduces differences in dose-volume histogram (DVH) metrics between alternative delineations, suggesting a washout effect. Conversely, NTCP metrics show an increase in differences between delineations as SV rises. This pattern holds true across various treatment plans, including 5-Beam IMRT, 9-Beam IMRT, and 2-Arc VMAT, as well as across different delineator combinations.

The accuracy required for delineation is case-specific,

influenced by factors beyond simple geometric variations. This underscores the need for personalized assessments in treatment planning to ensure optimal outcomes. Effective quality assurance (QA) programs must incorporate both geometrical variation analysis and dosimetric impact analysis to address the multifaceted challenges presented by delineation and setup variability in clinical practice.

Our findings also have significant implications for clinical workflows in radiotherapy. A nuanced understanding of how SV influences the clinical impact of DV necessitates careful evaluation and potential adjustment of treatment plans. Such adjustments are crucial to accommodate the varying degrees of SV and DV encountered in daily clinical practice.

In summary, this study provides pivotal insights into the complexities of the effects of delineations and delineation variation radiotherapy treatment planning. It emphasizes the importance of considering both setup and delineation variability in developing robust, effective, and personalized treatment strategies, to enhance the overall quality and efficacy of patient care in radiotherapy.

ACKNOWLEDGMENTS

This work was supported by National Cancer Institute (NCI) of the National Institute of Health under the award number R01CA222216. The content is solely the responsibility of the authors and does not necessarily represent the official views of the National Institutes of Health. We would like to thank Carina Medical, Radformation and Siemens Healthineers for providing us with AI delineations.

-
- [1] Shalini K. Vinod, Michael G. Jameson, Myo Min, and Lois C. Holloway. Uncertainties in volume delineation in radiation oncology: A systematic review and recommendations for future studies. *Radiotherapy and Oncology*, 121(2):169–179, 2016.
 - [2] Anup Kumar Bhardwaj, T.S. Kehwar, S.K. Chakarvarti, Goda Jayant Sastri, A.S. Oinam, Goswami Pradeep, Vinay Kumar, Mallick Indranil, and S.C. Sharma. Variations in inter-observer contouring and its impact on dosimetric and radiobiological parameters for intensity-modulated radiotherapy planning in treatment of localised prostate cancer. *Journal of Radiotherapy in Practice*, 7(2):77–88, 2008.
 - [3] Huijun Xu, J. James Gordon, and Jeffrey V. Siebers. Coverage-based treatment planning to accommodate delineation uncertainties in prostate cancer treatment. *Medical Physics*, 42(9):5435–5443, 2015.
 - [4] Claudio Fiorino, Michele Reni, Angelo Bolognesi, Giovanni Mauro Cattaneo, and Riccardo Calandrino. Intra- and inter-observer variability in contouring prostate and seminal vesicles: implications for conformal treatment planning. *Radiotherapy and Oncology*, 47(3):285–292, 1998.
 - [5] Hamidreza Nourzadeh, William T. Watkins, Mahmoud Ahmed, Cheukkai Hui, David Schlesinger, and Jeffrey V. Siebers. Clinical adequacy assessment of autocontours for prostate imrt with meaningful endpoints. *Medical Physics*, 44(4):1525–1537, 2017.
 - [6] Luciana Caravatta, Gabriella Macchia, Gian Mattiucci, Aldo Sainato, Nunzia LV Cernusco, Giovanna Mantello, Monica Di Tommaso, Marianna Trignani, Antonino De Paoli, Gianni Boz, Maria L Friso, Vincenzo Fusco, Marta Di Nicola, Alessio G Morganti, Domenico Genovesi, AG Morganti, M Massaccesi, G La Torre, L Caravatta, A Piscopo, R Tambaro, L Sofo, G Sallustio, M Ingrassio, G Macchia, F Deodato, V Picardi, E Ippolito, N Cellini, V Valentini, KA Goodman, C Hajj, B Asiyabola, A Gleisner, JM Herman, MA Choti, CL Wolfgang, M Swartz, BH Edil, RD Schulick, JL Cameron, TM Pawlik, T Yoshida, T Matsumoto, A Sasaki, K Shibata, M Aramaki, S Kitano, S Hishinuma, Y Ogata, M Tomikawa, I Ozawa, K Hirabayashi, S Igarashi, CH Crane, JA Antolak, II Rosen, KM Forster, DB Evans, NA Janjan, C Charnsangavej, PW Pisters, R Lenzi,

- MA Papagikos, RA Wolff, S Yovino, M Poppe, S Jabbour, V David, M Garofalo, N Pandya, R Alexander, N Hanna, WF Regine, L Caravatta, G Macchia, F Deodato, M Felicetti, F Cellini, A Ciabattini, M Buwenge, V Picardi, S Cilla, A Scapati, V Valentini, AG Morganti, C Fiorino, M Reni, A Bolognesi, GM Cattaneo, R Calandrino, TB Brunner, S Merkel, GG Grabenbauer, T Meyer, U Baum, T Papadopoulos, R Sauer, W Hohenberger, KA Goodman, WF Regine, LA Dawson, E Ben-Josef, K Haustermans, WR Bosch, J Turian, RA Abrams, W Sun, CN Leong, Z Zhang, JJ Lu, L Caravatta, G Salustio, F Pacelli, GD Padula, F Deodato, G Macchia, M Massaccesi, V Picardi, S Cilla, A Marinelli, N Cellini, V Valentini, AG Morganti, D Genovesi, G Ausili-C  faro, A Vinciguerra, A Augurio, M Di Tommaso, R Marchese, U Ricardi, AR Filippi, T Girinsky, K Di Biagio, M Belfiglio, E Barbieri, V Valentini, LR Dice, I Fotina, C L  tgendorf-Caucig, M Stock, R P  tter, D Georg, E Fokas, C Eccles, N Patel, KY Chu, S Warren, WG McKenna, TB Brunner, RA Abrams, KA Winter, WF Regine, H Safran, JP Hoffman, R Lustig, AA Kon-ski, AB Benson, JS Macdonald, TA Rich, CG Willett, CG Willett, J Moughan, E O'Meara, JM Galvin, CH Crane, K Winter, D Manfredi, TA Rich, R Rabinovitch, R Lustig, M Machtay, WJ Curran, VK Metha, EC Halperin, CA Perez, LW Brady, TB Brunner, U Baum, GG Grabenbauer, R Sauer, U Lambrecht, V Batumalai, ES Koh, GP Delaney, LC Holloway, MG Jameson, G Papadatos, DM Lonergan, S Crippa, S Partelli, M Falconi, H Yamazaki, K Nishiyama, E Tanaka, K Koiwai, N Shikama, Y Ito, S Arahira, T Tamamoto, T Shibata, Y Tamaki, T Kodaira, and M Oguchi. Inter-observer variability of clinical target volume delineation in radiotherapy treatment of pancreatic cancer: a multi-institutional contouring experience. *Radiation Oncology*, 9:198, 2014.
- [7] Jinzhong Yang, Harini Veeraghavan, Samuel G. Armato III, Keyvan Farahani, Justin S. Kirby, Jayashree Kalpathy-Kramer, Wouter van Elmpt, Andre Dekker, Xiao Han, Xue Feng, Paul Aljabar, Bruno Oliveira, Brent van der Heyden, Leonid Zamdborg, Dao Lam, Mark Gooding, and Gregory C. Sharp. Autosegmentation for thoracic radiation treatment planning: A grand challenge at aapm 2017. *Medical Physics*, 45(10):4568–4581, 2018.
- [8] P. F. Raudaschl, P. Zaffino, G. C. Sharp, M. F. Spadea, A. Chen, B. M. Dawant, T. Albrecht, T. Gass, C. Langguth, M. L  thi, F. Jung, O. Knapp, S. We-sarg, R. Mannion-Haworth, M. Bowes, A. Ashman, G. Guillard, A. Brett, G. Vincent, M. Orbes-Arteaga, D. C  rdenas-Pe  a, G. Castellanos-Dominguez, N. Agh-dasi, Y. Li, A. Berens, K. Moe, B. Hannaford, R. Schubert, and K. D. Fritscher. Evaluation of segmentation methods on head and neck CT: Auto-segmentation challenge 2015. *Med Phys*, 44(5):2020–2036, May 2017.
- [9] Paul J. Doolan, Stefanie Charalambous, Yiannis Rous-sakis, Agnes Leczynski, Mary Peratikou, Melka Benjamin, Konstantinos Ferentinos, Iosif Strouthos, Con-stantinos Zamboglou, and Efstratios Karagiannis. A clinical evaluation of the performance of five commercial artificial intelligence contouring systems for radiotherapy. *Frontiers in Oncology*, 13:1–13, 2023.
- [10] Andrea C. Lo, Mitchell Liu, Elisa Chan, Chad Lund, Pauline T. Truong, Shaun Loewen, Jeffrey Cao, Devin Schellenberg, Hannah Carolan, Tanya Berrang, Jonn Wu, Eric Berthelet, and Robert Olson. The impact of peer review of volume delineation in stereotactic body radiation therapy planning for primary lung cancer: A multicenter quality assurance study. *Journal of Thoracic Oncology*, 9(4):527–533, 2014.
- [11] Spencer Martin, Carol Johnson, Mark Brophy, David A. Palma, John L. Barron, Steven S. Beauchemin, Alexander V. Louie, Edward Yu, Brian Yaremko, Belal Ahmad, George B. Rodrigues, and Stewart Gaede. Impact of target volume segmentation accuracy and variability on treatment planning for 4d-ct-based non-small cell lung cancer radiotherapy. *Acta Oncologica*, 54(3):322–332, 2015. PMID: 25350526.
- [12] Carlos E. Cardenas, Jinzhong Yang, Brian M. Ander-son, Laurence E. Court, and Kristy B. Brock. Advances in auto-segmentation. *Seminars in Radiation Oncology*, 29(3):185–197, 2019. Adaptive Radiotherapy and Au-tomation.
- [13] Robert Poel, Elias R  fenacht, Evelyn Hermann, Stefan Scheib, Peter Manser, Daniel M. Aebbersold, and Mauricio Reyes. The predictive value of segmentation metrics on dosimetry in organs at risk of the brain. *Medical Image Analysis*, 73:102161, 2021.
- [14] Minsong Cao, Bradley Stiehl, Victoria Y. Yu, Ke Sheng, Amar U. Kishan, Robert K. Chin, Yingli Yang, and Dan Ruan. Analysis of geometric performance and dosimet-ric impact of using automatic contour segmentation for radiotherapy planning. *Frontiers in Oncology*, 10, 2020.
- [15] Tze Yee Lim, Erin Gillespie, James Murphy, and Kevin L. Moore. Clinically oriented contour evaluation using dosimetric indices generated from automated knowledge-based planning. *International Journal of Radiation On-cology Biology Physics*, 103:1251–1260, 2019.
- [16] A. Smolders, E. Choulilitsa, K. Czerska, N. Bizzocchi, R. Krcek, A. Lomax, D. C. Weber, and F. Albertini. Dosimetric comparison of autocontouring techniques for online adaptive proton therapy. *Physics in Medicine and Biology*, 68, 2023.
- [17] Ward van Rooij, Max Dahele, Hugo Ribeiro Brandao, Alexander R. Delaney, Berend J. Slotman, and Wilko F. Verbakel. Deep learning-based delineation of head and neck organs at risk: Geometric and dosimetric evalua-tion. *International Journal of Radiation Oncology Biol-ogy Physics*, 104:677–684, 2019.
- [18] Nelson Tsz Cheong Fung, Wai Man Hung, Chun Kin Sze, Michael Chi Hang Lee, and Wai Tong Ng. Automatic seg-mentation for adaptive planning in nasopharyngeal carcinoma imrt: Time, geometrical, and dosimetric analysis. *Medical Dosimetry*, 45:60–65, 2020.
- [19] Hongbo Guo, Jiazhou Wang, Xiang Xia, Yang Zhong, Jiayuan Peng, Zhen Zhang, and Weigang Hu. The dosi-metric impact of deep learning-based auto-segmentation of organs at risk on nasopharyngeal and rectal cancer. *Radiation Oncology*, 16:1–14, 2021.
- [20] Walter R. Bosch, William L. Straube, John W. Matthews, and James A. Purdy. *Data From Head-Neck_Cetuximab. The Cancer Imaging Archive*, 2015.
- [21] K. Kian Ang, Qiang Zhang, David I. Rosenthal, Phuc Fel-ix Nguyen-Tan, Eric J. Sherman, Randal S. Weber, James M. Galvin, James A. Bonner, Jonathan Harris, Adel K. El-Naggar, Maura L. Gillison, Richard C. Jor-dan, Andre A. Kanski, Wade L. Thorstad, Andy Trotti, Jonathan J. Beitler, Adam S. Garden, William J. Spanos, Sue S. Yom, and Rita S. Axelrod. Randomized phase

- iii trial of concurrent accelerated radiation plus cisplatin with or without cetuximab for stage iii to iv head and neck carcinoma: Rtog 0522. *Journal of Clinical Oncology*, 32(27):2940–2950, 2014. PMID: 25154822.
- [22] Martin Vallières, Emily Kay-Rivest, Léo Jean Perrin, Xavier Liem, Christophe Furstoss, Nader Khaouam, Phuc Félix Nguyen-Tan, Chang-Shu Wang, and Khalil Sultanem. *Data from Head-Neck-PET-CT. The Cancer Imaging Archive*, 2017.
- [23] Martin Vallières, Emily Kay-Rivest, Léo Jean Perrin, Xavier Liem, Christophe Furstoss, Hugo J. W. L. Aerts, Nader Khaouam, Phuc Felix Nguyen-Tan, Chang-Shu Wang, Khalil Sultanem, Jan Seuntjens, and Issam El Naqa. Radiomics strategies for risk assessment of tumour failure in head-and-neck cancer. *Scientific Reports*, 7(1):10117, Aug 2017.
- [24] Hao Tang. Uanet github repository. <https://github.com/uci-cbcl/UaNet>. Last Accessed: 2023-04-23.
- [25] Hao Tang, Xuming Chen, Yang Liu, Zhipeng Lu, Junhua You, Mingzhou Yang, Shengyu Yao, Guoqi Zhao, Yi Xu, Tingfeng Chen, Yong Liu, and Xiaohui Xie. Clinically applicable deep learning framework for organs at risk delineation in CT images. *Nature Machine Intelligence*, 1(10):480–491, sep 2019.
- [26] C. L. Brouwer, R. J. Steenbakkers, J. Bourhis, W. Budach, C. Grau, V. Grégoire, M. van Herk, A. Lee, P. Maingon, C. Nutting, B. O’Sullivan, S. V. Porceddu, D. I. Rosenthal, N. M. Sijtsema, and J. A. Langendijk. CT-based delineation of organs at risk in the head and neck region: DAHANCA, EORTC, GORTEC, HKN-PCSG, NCIC CTG, NCRI, NRG Oncology and TROG consensus guidelines. *Radiother Oncol*, 117(1):83–90, Oct 2015.
- [27] Radformation Inc. Autocontour.
- [28] Carina Medical. Intcontour.
- [29] Google Inc. Surface distance, 2018.
- [30] C. Burman, G.J. Kutcher, B. Emami, and M. Goitein. Fitting of normal tissue tolerance data to an analytic function. *International Journal of Radiation Oncology*Biophysics*, 21(1):123–135, 1991. Three-Dimensional Photon Treatment Planning Report of the Collaborative Working Group on the Evaluation of Treatment Planning for External Photon Beam Radiotherapy.
- [31] J. J. Gordon, N. Sayah, E. Weiss, and J. V. Siebers. Coverage optimized planning: Probabilistic treatment planning based on dose coverage histogram criteria. *Medical Physics*, 37(2):550–563, 2010.
- [32] Andrzej Niemierko and Michael Goitein. Calculation of normal tissue complication probability and dose-volume histogram reduction schemes for tissues with a critical element architecture. *Radiotherapy and Oncology*, 20(3):166–176, 1991.
- [33] Hang Min, Jason Dowling, Michael G Jameson, Kirrily Cloak, Joselle Faustino, Mark Sidhom, Jarad Martin, Martin A Ebert, Annette Haworth, Phillip Chlap, Jeremiah de Leon, Megan Berry, David Pryor, Peter Greer, Shalini K Vinod, and Lois Holloway. Automatic radiotherapy delineation quality assurance on prostate mri with deep learning in a multicentre clinical trial. *Physics in Medicine & Biology*, 66(19):195008, sep 2021.
- [34] Jue Jiang, Yuchi Hu, Chia-Ju Liu, Darragh Halpenny, Matthew Hellmann, Joseph Deasy, Gig Mageras, and Harini Veeraraghavan. Multiple resolution residually connected feature streams for automatic lung tumor segmentation from ct images. *IEEE Transactions on Medical Imaging*, PP:1–1, 07 2018.
- [35] Lawrence B. Marks, Søren M. Bentzen, Joseph O. Deasy, Feng-Ming Spring Kong, Jeffrey D. Bradley, I. Vogelius, Issam El Naqa, Jessica L. Hubbs, Joos V. Lebesque, Robert Timmerman, Mary K. Martel, and Andrew Jackson. Radiation dose-volume effects in the lung. *Int J Radiat Oncol Biol Phys.*, 76(3), Mar 2010.
- [36] Therapy Physics Committee AAPM Task Group 166. *The Use and QA of Biologically Related Models for Treatment Planning Report of AAPM Task Group 166*. American Association of Physicists in Medicine, 2012.
- [37] X. Allen Li, Markus Alber, Joseph O. Deasy, Andrew Jackson, Kyung Wook Ken Jee, Lawrence B. Marks, Mary K. Martel, Charles Mayo, Vitali Moiseenko, Alan E. Nahum, Andrzej Niemierko, Vladimir A. Semenenko, and Ellen D. Yorke. The use and qa of biologically related models for treatment planning: Short report of the tg-166 of the therapy physics committee of the aapm. *Medical Physics*, 39:1386–1409, 2012.
- [38] Bradley. Efron, Robert. Tibshirani, and Taylor & Francis. *An introduction to the bootstrap*. Chapman & Hall, New York ; London, 1993.
- [39] PhD Kendrick Kay. Probability distributions and error bars - statistics and data analysis in matlab, 2014.
- [40] Eric Aliotta, Hamidreza Nourzadeh, and Jeffrey Siebers. Quantifying the dosimetric impact of organ-at-risk delineation variability in head and neck radiation therapy in the context of patient setup uncertainty. *Physics in Medicine & Biology*, 64(13):135020, jul 2019.
- [41] Ji Zhu, Xinyuan Chen, Bining Yang, Nan Bi, Tao Zhang, Kuo Men, and Jianrong Dai. Evaluation of automatic segmentation model with dosimetric metrics for radiotherapy of esophageal cancer. *Frontiers in Oncology*, 10:1–9, 2020.
- [42] L. Hoffmann, G. F. Persson, L. Nygård, T. B. Nielsen, S. Borrisova, F. Gaard-Petersen, M. Josipovic, A. A. Khalil, R. Kjeldsen, M. M. Knap, C. Kristiansen, D. S. Møller, W. Ottosson, H. Sand, R. Thing, M. Pøhl, and T. Schytte. Thorough design and pre-trial quality assurance (qa) decrease dosimetric impact of delineation and dose planning variability in the strictlung and starlung trials for stereotactic body radiotherapy (sbrt) of central and ultra-central lung tumours. *Radiotherapy and Oncology*, 171:53–61, 2022.